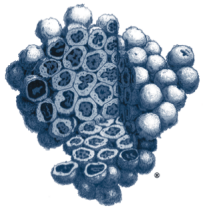

STEM CELLS®

Coordinated Changes of Mitochondrial Biogenesis and Antioxidant Enzymes during Osteogenic Differentiation of Human Mesenchymal Stem Cells

Chien-Tsun Chen, Yuru V. Shih, Tom K. Kuo, Oscar K. Lee and Yau-Huei Wei

Stem Cells published online Jan 24, 2008;
DOI: 10.1634/stemcells.2007-0509

Stem Cells Express, published online January 24, 2008; doi:10.1634/stemcells.2007-0509

STEM CELLS®

TISSUE-SPECIFIC STEM CELLS

Coordinated Changes of Mitochondrial Biogenesis and Antioxidant Enzymes during Osteogenic Differentiation of Human Mesenchymal Stem Cells

Chien-Tsun Chen[1], Yuru V. Shih[2], Tom K. Kuo[2], Oscar K. Lee[3,4], Yau-Huei Wei[1]

[1]Institute of Biochemistry and Molecular Biology, National Yang-Ming University, Taipei 112, Taiwan; [2]Institute of Biopharmaceutical Sciences, National Yang-Ming University, Taipei 112, Taiwan; [3]Institute of Clinical Medicine, National Yang-Ming University, Taipei 112, Taiwan; and [4]Department of Medical Research and Education, Taipei Veterans General Hospital, Taipei 112, Taiwan

Key Words. Mesenchymal stem cells • Osteogenic differentiation • Mitochondria • Metabolic switch • Antioxidant enzymes

ABSTRACT

The multi-differentiation ability of mesenchymal stem cells (MSCs) holds great promise for cell therapy. Numerous studies have focused on the establishment of differentiation protocols while little attention has been paid to the metabolic changes during the differentiation process. Mitochondria, the powerhouse of mammalian cells, vary in their number and function in different cell types with different energy demands; but how these variations are associated with cell differentiation remains elusive. In this study, we investigated the changes of mitochondrial biogenesis and bioenergetic function using human MSCs (hMSCs) because of their well-defined differentiation potentials. Upon osteogenic induction, the copy number of mitochondrial DNA, protein subunits of the respiratory enzymes, oxygen consumption rate, and intracellular ATP content were increased, indicating the upregulation of aerobic mitochondrial metabolism. On the other hand, undifferentiated hMSCs showed higher levels of glycolytic enzymes and lactate production rate, suggesting that hMSCs rely more on glycolysis for energy supply in comparison with hMSC-differentiated osteoblasts. In addition, we observed a dramatic decrease of intracellular reactive oxygen species (ROS) as a consequence of upregulation of two antioxidant enzymes, Mn-dependent superoxide dismutase and catalase. Finally, we found that exogenous H_2O_2 and mitochondrial inhibitors could retard the osteogenic differentiation. These findings suggested an energy production transition from glycolysis to oxidative phosphorylation in hMSCs upon osteogenic induction. Meanwhile, antioxidant enzymes were concurrently upregulated to prevent the accumulation of intracellular ROS. Together, our

Correspondence: should be sent to Prof. Yau-Huei Wei or Dr. Oscar K. Lee, Professor Yau-Huei Wei., 155 Li-Nong St., Sec. 2, Peitou, Taipei 112, Taiwan, E-mail address:joeman@ym.edu.tw (YH Wei), Tel:+886-2-28267118 , Fax:+886-2-28264843, Dr. Oscar K. Lee, 201 Shi-Pai Rd., Sec. 2, Taipei 112, Taiwan, E-mail address:kslee@vghtpe.gov.tw (OK Lee), Tel:+886-2-28757557, Fax:+886-2-28757657; Acknowledgement: National Science Council of Taiwan, Ministry of Education, Executive Yuan, Taiwan, and Taipei Veterans General Hospital; Received July 02, 2007; accepted for publication January 04, 2008; first published online in Stem Cells Express January 24, 2008. 1066-5099/2008/$30.00/0 doi: 10.1634/stemcells.2007-0509

findings suggest that coordinated regulation of mitochondrial biogenesis and antioxidant enzymes occurs synergistically during osteogenic differentiation of hMSCs.

INTRODUCTION

Adult human mesenchymal stem cells (hMSCs) are somatic stem cells residing in a variety of tissues [1], and they can differentiate into progenies of multiple lineages including osteoblasts, chondrocytes, adipocytes and hepatocytes. Numerous efforts have been made not only to uncover the mechanisms of stemness and multi-differentiation ability of hMSCs, but also to test their potential for cell therapy and gene therapy in a number of human diseases [2]. However, little attention has been paid to the alterations in energy metabolism and cellular redox status during differentiation [3]. Recent studies revealed that murine embryonic stem cells (ESCs) express high levels of glycolytic enzymes and low mitochondrial oxygen consumption [4], indicating a great difference in energy production between stem cells and terminally differentiated somatic cells. Besides, it has been reported that the intracellular distribution of mitochondria is associated with the degree of stemness of adult monkey stromal stem cells [5]. These findings have pointed out a possible role of mitochondria and the bioenergetic functions in stem cells and their differentiated progenies.

Mitochondria are the organelles where many vital metabolic reactions take place. They are also called the power plant of mammalian cells because a majority of ATP is generated through the mitochondrial electron transport chain, in which a proton gradient is generated across the inner membrane by respiratory Complexes I, III and IV, and then driving ATP synthesis through Complex V (ATP synthase) [6]. Another important feature of mitochondria is that they harbor their own genome called mitochondrial DNA (mtDNA), which contains 16,569 base pairs of nucleotides in a circular double-stranded structure, encoding 2 rRNAs, 22 tRNAs and 13 polypeptides [7]. However, the crosstalk between the mitochondrial and nuclear genomes in terms of the maintenance of normal cellular function such as proliferation and differentiation still remains elusive [8].

Apart from their bioenergetic functions, mitochondria are also the major source of endogenous reactive oxygen species (ROS) in human cells because a small portion of electrons constantly leak out from electron transport chain and contribute to the production of mitochondrial ROS, a deleterious by-product of aerobic metabolism causing oxidative damage to DNA, proteins and lipids [9, 10]. Elevated levels of ROS can cause a variety of human diseases such as cardiovascular diseases, ischemia/reperfusion injuries, neurological disorders, diabetes and cancer as a consequence of tissue damages. To overcome the detrimental effects of ROS, there is an array of defense systems including enzymatic and non-enzymatic antioxidants in intra- and extra-cellular spaces to protect cells from the attack of ROS [11]. The leaked-out electrons of electron transport chain react with oxygen to form superoxide anions ($O_2^{\cdot-}$), which can be converted by superoxide dismutase (SOD) to

hydrogen peroxide (H_2O_2), followed by further decomposition to H_2O and O_2 by catalase and glutathione peroxidase [12, 13]. Since ROS also serves as a second messenger in signal transduction, production of ROS and the activities of antioxidant enzymes must be tightly controlled to maintain the homeostasis of the intracellular redox status so that proper ROS-mediated signaling can take place without elevating intracellular oxidative stress.

The density and activity of mitochondria vary in different types of terminally differentiated cells. However, little is known regarding how this diversity is controlled during the developmental processes of an organism from a single embryo. Lack of clear understanding of the inter-genomic communication in this process necessitates the investigation of the mechanisms underlying the regulation of mitochondrial biogenesis during cellular differentiation and maturation. Therefore, we took advantage of the well-established osteogenic differentiation system of hMSCs to dissect changes in cellular bioenergetic functions [14]. We hypothesized that mitochondrial functions are altered in response to osteogenic differentiation signals. In this study, we found that during osteogenic differentiation of hMSCs, mtDNA copy number, protein subunits of respiratory enzymes, oxygen consumption rate, intracellular ATP level and antioxidant enzymes are positively regulated while the intracellular ROS is suppressed, demonstrating a well-coordinated process involving upregulation of the biogenesis and respiratory function of mitochondria and expression of antioxidant enzymes.

MATERIALS AND METHODS

Culture of bone marrow hMSCs and *in vitro* osteogenic induction

Cultures of bone marrow hMSCs were established from the bone marrow aspirates of five healthy donors (between 20 and 50 years old) undergoing fracture fixation surgery after the approval of the Institutional Review Board and informed consent as previously reported [15, 16]. All the experiments described below, except the lactate release and MnSOD protein expression measurements presented in the supplement, were carried out using hMSCs from a 28-year-old donor 1. Cells were cultured in Iscove's modified Dulbecco's medium (IMDM) (Gibco BRL, Invitrogen, Grand Island, NY) consisting of 10% fetal bovine serum (Hyclone, Logan, UT), 10 ng/ml bFGF, 10 ng/ml EGF, 100 units/ml penicillin, 100 μg/ml streptomycin and 2 mM L-glutamine (Gibco BRL) at 37°C in a humidified chamber containing 5% CO_2. Osteogenic induction was carried out by incubating hMSCs in an induction medium composed of serum-free IMDM, 0.1 μM dexamethasone, 10 mM β-glycerol phosphate, 0.2 mM ascorbic acid (Sigma-Aldrich, St. Louis, MO), 100 units/ml penicillin and 100 μg/ml streptomycin.

Alkaline phosphatase assay

For alkaline phosphatase (ALP) staining, cells in 35-mm dishes were fixed with 4% paraformaldehyde and stained with 5-bromo-4-chloro-3-indolyl phosphate/nitroblue tetrazolium (BCIP/NBT) (Sigma-Aldrich). ALP activity was assayed as previously described [17]. Cells in 96-well plates were lysed with 0.05% SDS at 37°C for

10 min and incubated in a solution containing 8 mM 4-nitrophenyl phosphate and 2 mM $MgCl_2$ in 2-amino-2-methyl-1-propanol (Sigma-Aldrich) for 30 min in the dark at 37°C. The reaction was stopped with 0.02 N NaOH and the absorbance at 405 nm was measured by an ELISA reader (Power Wave HT 340, Bio-Tek, Cumbria, England). To examine the effect of H_2O_2 or oligomycin on osteogenic differentiation, hMSCs were treated two days post osteogenic induction and the ALP activity was determined on the fifth day of induction.

RNA extraction and RT-QPCR

RNA was extracted with TRI Reagent (Sigma-Aldrich) and 5 μg RNA was reverse-transcribed to cDNA with the Ready-to-Go RT-PCR kit (Amersham Biosciences, Uppsala, Sweden). Quantitative PCR analysis was performed using the LightCycler Taqman Master kit (Roche Applied Sciences, Mannheim, Germany) according to the manufacturer's instructions. Gene expression levels were normalized by the house-keeping gene, glyceraldehyde 3-phosphate dehydrogenase (GAPDH). Information of the primer pairs and probes are listed in Table S1.

Measurement of mitochondrial mass

Mitochondrial mass was measured as previously described [18]. Cells were incubated in fresh medium with 2.5 μM nonyl acridine orange (NAO, Molecular Probes, Eugene, OR) for 10 min at 25°C in the dark and harvested in a solution containing 5 mM KCl, 140 mM NaCl, 2 mM $CaCl_2$, 1 mM $MgCl_2$, 10 mM glucose and 5 mM HEPES buffer (pH 7.4). The fluorescence intensity of 10,000 cells was recorded on a flow cytometer (Model EPICS XL-MCL, Beckman-Coulter, Miami, FL) with the excitation wavelength at 488 nm and emission wavelength at 535 nm.

Determination of relative mtDNA copy number

An aliquot of 50 ng DNA was subjected to quantitative PCR using LightCycler-FastStar DNA Master SYBR Green I kit (Roche Applied Sciences). DNA fragments of ND1 gene (mtDNA-encoded) and β-actin gene (nuclear DNA-encoded, served as internal control) were amplified with specific primer pairs (Table S1), respectively. The relative mtDNA copy number was measured by normalization of the crossing points in quantitative PCR curves between ND1 and β-actin genes using the RelQuant software (Roche Applied Sciences). PCR was performed as follows: one cycle of hot start at 95°C for 10 min, 35 cycles of 5 sec denaturation at 95°C, 10 sec annealing at 58°C, and 20 sec extension at 72°C.

Western blot analysis

An aliquot of 25 μg proteins were separated on a 12% SDS-PAGE gel and blotted onto a PVDF membrane (Amersham Biosciences). Nonspecific bindings were blocked by 3% skim milk in TBST buffer (50 mM Tris-HCl, 150 mM NaCl, 0.1% Tween 20, pH 7.4) and the membrane was blotted with indicated primary antibodies (Table S2). After incubation with a HRP-conjugated secondary antibody the protein intensity was determined by an ECL chemiluminescence reagent (Perkin-Elmer Life Sciences, Inc., Boston, MA).

Measurement of oxygen consumption

Oxygen consumption rate was measured by the 782 Oxygen Meter (Strathkelvin Instruments, Scotland, UK). An aliquot of 5 x 10^5 cells were incubated on ice for 10 min in 330 µl assay buffer (125 mM sucrose, 65 mM KCl, 2 mM $MgCl_2$, 20 mM phosphate buffer, pH 7.2) containing 0.0003% digitonin (Sigma-Aldrich) to permeabilize the mitochondrial outer membrane. The cell suspension was then transferred into the incubation chamber and oxygen consumption rate was measured after injection of 6 mM succinate into the chamber as the electron donor.

Measurement of lactate production rate

Lactate production rate was measured by a Lactate Reagent kit (Trinity Biotech plc, Wicklow, Ireland). Cells in 6-well plates were replenished with fresh medium and incubated for 8 hr. An aliquot of 10 µl medium was then transferred to a 96-well plate to mix with the Lactate Reagent and the absorbance at 540 nm was measured by an ELISA reader (Power Wave HT 340). The absorbance was then normalized by total cell number and divided by the time of incubation.

Measurement of intracellular ATP content

Intracellular ATP level was measured by the Bioluminescent Somatic Cell Assay Kit (Sigma-Aldrich). An aliquot of 50 µl viable cell suspension was mixed with 150 µl Somatic Cell Releasing Reagent to release the intracellular ATP. Half of the mixture was then transferred into a black OptiPlate™-96F 96-well plate (Packard Biosciences, Groningen, The Netherlands) containing 100 µl ATP Assay Mix and the luminescence intensity was measured by the Victor^2™ 1420 Multilabel Counter (Perkin-Elmer Life Sciences, Inc.). The luminescence intensity was then divided by total cell number.

alamarBlue™ cell viability assay

Cells in 96-well plates were incubated with fresh medium containing 1x alamarBlue™ cell viability assay reagent (AbD Serotec Ltd., Oxford, UK) at 37°C for 4 hr. The fluorescence intensity was measured by the Victor^2™ 1420 Multilabel Counter (Perkin-Elmer Life Sciences, Inc.) with the excitation wavelength at 538 nm and emission wavelength at 590 nm.

Determination of intracellular ROS

For measurement of H_2O_2 and $O_2^{\cdot-}$ levels, cells were incubated in a medium containing 40 µM 2',7'-dichlorodihydrofluorescein diacetate and 5 µg/ml hydroethidine (Molecular Probes), respectively, at 37°C in the dark for 10 min. Cells were then resuspended in 50 mM HEPES buffer and the fluorescence intensity of 10,000 cells was recorded on a flow cytometer (Model EPICS XL-MCL) with the excitation wavelength at 488 nm and emission wavelength at 535 nm and 580 nm, respectively.

Activity assay of catalase and total SOD

Catalase activity was determined by monitoring the rate of decomposition of H_2O_2 from the decrease in absorbance at 240 nm [10]. Total SOD activity was assayed by monitoring nitroblue tetrazolium (NBT) reduction according to Spitz and Oberley [19] with some modifications. SOD inhibits NBT reduction caused by $O_2^{\cdot-}$ in the aerobic xanthine/xanthine oxidase system, and changes of absorbance at 560 nm within 2 min were recorded. One unit of

SOD is defined as the amount of enzyme that causes 45% inhibition of NBT reduction under the assay condition described [10].

Statistical analysis

Statistical analysis was performed using the SPSS Programs for Windows, Standard Version (version 10.0.1). The data are presented as means ± standard deviation of the results from three independent experiments. The significance level was determined by nonparametric Mann-Whitney U test. A difference is considered to be statistically significant when p value < 0.05.

RESULTS

Osteogenic induction of hMSCs

After growing in osteogenic induction medium, hMSCs underwent distinct morphological changes from fibroblast-like (Fig. 1A) to flattened and polygonal cells and showed positive staining of ALP (Fig. 1B). By spectrophotometric assay, ALP activity was detectable as early as four days after osteogenic induction and was increased in a time-dependent manner (Fig. 1C). Osteogenic marker genes such as Core-binding factor a-1 (Cbfa-1), osteocalcin (OCA), osteonectin (ONT) and osteopontin (OPT) were upregulated after induction (Fig. 1D). These findings indicate that hMSCs could be induced to differentiate into osteoblasts under defined culture conditions.

Increase in mtDNA copy number, but not mitochondrial mass, after osteogenic induction

To investigate the alterations of mitochondria in differentiation, we first analyzed changes in mitochondrial mass and mtDNA copy number throughout the osteogenic induction period for up to four weeks. No significant change in mitochondrial mass was observed except for a short-term decrease (down to 80.5 ± 3.7% of undifferentiated hMSCs, $p < 0.05$) on the first day of induction, which resumed to the initial level thereafter (Fig. 2A). By contrast, determination of mtDNA copy number by real-time PCR revealed a dynamic change with an initial decline (66.0 ± 2.8% on day 4) upon osteogenic induction, followed by a subsequent increase (up to 137.0 ± 9.6% on day 28) after the fourth day of induction (Fig. 2A). Despite the relatively stable level of mitochondrial mass during osteogenic differentiation, the significant increase of mtDNA content suggests a possible increase in the biosynthesis of mitochondrial respiratory enzymes resulting from the increase of the mitochondrial genome.

Increase in the expression of respiratory enzymes and oxygen consumption rate during osteogenic induction

Recent studies indicated that anaerobic glycolysis provides most of the energy for murine ESCs [4]. To investigate whether aerobic metabolism would gradually become dominant during osteogenic differentiation, we analyzed the expression levels of protein subunits of respiratory enzyme complexes. By Western blot analysis, we found a significant increase in the protein levels of core I subunit of Complex III (3.14 ± 1.15 fold), cytochrome

oxidase subunit I (COX I, 3.54 ± 1.16 fold) of Complex IV and β subunit of Complex V (1.70 ± 0.11 fold) (Fig. 2B). In addition, a slight increase of the expression levels of iron-sulfur protein 3 of Complex I (1.26 ± 0.44 fold) and succinate dehydrogenase subunit A (SDHA) of Complex II (1.53 ± 0.39 fold) was also noted (Fig. 2B). The increase in the amount of protein subunits of respiratory enzymes suggests that mitochondrial biogenesis was enhanced in relation to the increase of mtDNA copy number during osteogenic differentiation. To determine the activities of aerobic metabolism, we measured the oxygen consumption rate by the 782 Oxygen Meter (Strathkelvin Instrument). We observed a significant increase of oxygen consumption rate of 2-week differentiated osteoblasts (ost2w) compared with undifferentiated hMSCs (Fig. 2C; 3.2 ± 0.7 fold, $p < 0.01$), indicating enhanced mitochondrial respiration. These observations indicate that mitochondria became more active, as the amounts of mtDNA and respiratory enzymes were increased, which resulted in an elevation of the aerobic metabolism during osteogenic differentiation of hMSCs.

Upregulation of mitochondrial biogenesis-associated genes

To further explore the underlying mechanism involved in the enhancement of mitochondrial respiratory function, we examined the mRNA expression levels of three crucial genes associated with mitochondrial biogenesis including mitochondrial transcription factor A (mtTFA), DNA polymerase γ (Pol γ), and PPARγ coactivator-1α (PGC-1α. By real-time PCR, we observed a gradual increase of mtTFA and Pol γ expression along with the osteogenic differentiation and the changes reached the plateau at around day 21 (Fig. 2D; mtTFA, 4.6 ± 1.1; Pol γ, 4.9 ± 0.9 fold). PGC-1α showed a more dynamic expression pattern with a peak expression level on day 7 (14.8 ± 5.9 fold).

Decrease in the expression of glycolytic enzymes and lactate production rate during osteogenic induction

Since the mitochondrial respiratory activity was augmented, it raised another question as to whether the glycolytic activity was changed. By Western blot analysis, we found a significant decrease in the protein levels of glucophosphate isomerase (GPI, 0.59 ± 0.13 fold) and phosphofructokinase (PFK, 0.63 ± 0.20 fold) in ost2w cells (Fig. 3A). On the other hand, the protein level of pyruvate dehydrogenase (PDH), an enzyme which is responsible for converting pyruvate into acetyl CoA to enter TCA cycle and aerobic metabolism, was dramatically increased (2.19 ± 1.31 fold). In addition, PDH kinase (PDK), which can phosphorylate PDH to inhibit its activity, was found to be significantly decreased (< 0.10 fold). We also measured the lactate production rate and found that undifferentiated hMSCs had a higher lactate production rate compared with ost2w (Fig. 3B; 941.6 ± 79.0 vs. 503.2 ± 32.3 ng/10^4 cells/hr, $p < 0.01$), indicating profound anaerobic glycolytic metabolism in hMSCs. Consequently, the intracellular ATP content of hMSCs was measured and we found that intracellular ATP content was initially decreased (17.8 ± 2.9 pmol/cell) on the second day of induction in comparison with undifferentiated hMSCs (23.6 ± 2.9 pmol/cell), and was subsequently increased to 1.5 times of that of control (35.7 ± 4.6 pmol/cell) on the

fourth day of induction and maintained stably thereafter (Fig. 3C).

Higher dependence on glycolysis of hMSCs versus mitochondrial respiration of hMSCs-differentiated osteoblasts

To further characterize the switch of energy generation from glycolysis to mitochondrial oxidative phosphorylation during osteogenic differentiation, hMSCs and ost2w were treated with two glycolytic inhibitors (iodoacetamide and 2-deoxy- glucose) and two mitochondrial respiratory inhibitors (antimycin A, Complex III inhibitor; and oligomycin, Complex V inhibitor) to compare their dependence on the two metabolic pathways using cell viability as readouts. hMSCs showed significantly lower viability in comparison with ost2w after treatment with both iodoacetamide and 2-deoxy-glucose for 24 hr (Figs. 4A and 4B). On the contrary, ost2w showed significantly lower viability after treatment with antimycin A or oligomycin. (Figs. 4C and 4D). These results suggest that hMSCs were more glycolysis-dependent in energy supply while differentiated osteoblasts were more mitochondrial respiration-dependent.

Dramatic reduction of intracellular ROS and upregulation of antioxidant enzymes upon osteogenic induction

Since enhanced mitochondrial biogenesis and aerobic metabolism were associated with osteogenic differentiation, we further investigated whether the undesired toxic by-products, ROS were concurrently produced during osteogenic differentiation. Surprisingly, intracellular levels of H_2O_2 and $O_2^{\cdot -}$ were dramatically reduced as early as the second day of osteogenic induction (Fig. 5A; H_2O_2: 32.5 ± 3.9%; $O_2^{\cdot -}$: 72.0 ± 7.6% of undifferentiated hMSCs, $p < 0.05$). However, as osteogenic differentiation went on, gradual rebound of H_2O_2 and $O_2^{\cdot -}$ was noted. H_2O_2 was resumed to 62.8 ± 18.2% and $O_2^{\cdot -}$ level was slightly higher than that of undifferentiated hMSCs (113.7 ± 13.0%) after 28 days of induction. The unexpected decline of intracellular ROS directed us to ask whether this phenomenon was caused by the changes in the antioxidant capacity of hMSCs during differentiation. We found that protein levels of MnSOD and catalase were upregulated significantly in a time-dependent manner during osteogenic differentiation, but no such change was observed in Cu/ZnSOD (Fig. 5B). Quantification by densitometry revealed that the amounts of catalase and MnSOD were increased to about 3 and 4 folds, respectively, after 14 days of induction (Fig. 5C). We also measured the levels of other proteins of the antioxidant defense system including glutathione reductase (GR), glutathione peroxidase (GPx), peroxiredoxin-I (Prx-I), peroxiredoxin-III (Prx-III), thioredoxin-I (Trx-I) and thioredoxin reductase (TrxR) by Western blot analysis but no significant differences in any of these proteins were noted (data not shown). These results indicate that during osteogenic differentiation, only few enzymes of the antioxidant defense system are strongly upregulated in hMSCs to reduce endogenous ROS.

Increase in antioxidative capacity of hMSCs after osteogenic differentiation

To further confirm the changes of antioxidative capacity after osteogenic differentiation of

hMSCs, catalase and total SOD activities were measured. Both enzyme activities were significantly increased in ost2w (Figs. 6A and 6B; catalase: 68.0 ± 11.2 vs. 12.0 ± 3.7, $p < 0.05$; total SOD: 231.7 ± 43.1 vs. 66.7 ± 10.8 unit/mg protein, $p < 0.05$). We further examined their resistance to exogenous ROS stress by cell viability assay. After incubating hMSCs and ost2w with different doses of H_2O_2 and menadione, which can generate $O_2^{\cdot -}$, significant reduction in the viability of hMSCs was observed in both treatments (Figs. 6C and 6D). Upon treatment with as high as 750 μM H_2O_2, the viability of hMSCs was 50.8 ± 1.5% while that of ost2w was 97.1 ± 16.4%. Upon treatment with 25 μM menadione, the viability of hMSCs was 15.2 ± 4.3% while that of ost2w was 37.7 ± 4.0%. These results indicate that the antioxidative capacity has been increased during the osteogenic differentiation of hMSCs.

Inhibitory effects of H_2O_2 and oligomycin on osteogenic differentiation of hMSCs

Based on the observations of enhanced mitochondrial biogenesis and upregulation of antioxidant enzymes, we speculated that during osteogenic differentiation, hMSCs switched their preference of energy production from glycolysis to oxidative phosphorylation, which is much more efficient in generating ATP. Therefore, we investigated whether alterations of intracellular ROS levels and mitochondrial activity by exogenous addition of H_2O_2 and oligomycin would affect osteogenic differentiation of hMSCs. hMSCs were induced to undergo osteogenic differentiation for two days and then treated with sublethal doses of H_2O_2 or oligomycin. ALP activities and Cbfa-1 mRNA expression levels were examined as indicators of osteogenic differentiation. After treatment with 125-500 μM H_2O_2, hMSCs showed significantly reduced ALP activity compared with untreated control on the fifth day of induction (Fig. 7A). Similarly, after treatment with 2.5μg/ml oligomycin, hMSCs showed significantly reduced ALP activity (Fig. 7B). We also observed reduced levels of Cbfa-1 mRNA expression in four-week differentiated hMSCs by treatment with H_2O_2 or oligomycin (Fig. 7C). These results indicate that excess ROS or decreased mitochondrial oxidative phosphorylation could hamper the osteogenic differentiation of hMSCs.

DISCUSSION

In the present study, we showed that during osteogenic differentiation of hMSCs, mtDNA copy number, protein levels of respiratory enzymes, oxygen consumption rate, mRNA levels of mitochondrial biogenesis-associated genes and intracellular ATP content were increased along with the dramatic decline of intracellular ROS as well as upregulation of antioxidant enzymes. These observations indicate that in hMSCs, mitochondria are maintained at a relatively low activity level, and upon osteogenic induction, mitochondrial respiratory functions are increased in response to a higher energy demand. In a recent study, Cho *et al*. [20] also observed dynamic changes of mitochondrial biogenesis and antioxidant enzymes during the spontaneous differentiation of hESCs. However, spontaneous differentiation of hESCs gives rise to embryoid bodies consisting of cells of all three germ layers, in which lineage-specific regulations in metabolic activities and bioenergetic functions

can be masked. In this study, we used osteogenic differentiation of hMSCs as a model, in which defined lineage-specific differentiation process occurred and the changes of metabolic activities and bioenergetic functions of mitochondria could be precisely delineated.

The intergenomic communication between mitochondrial and nuclear genomes in stem cells is complicated and remains elusive [21]. The increase in the copy number of mtDNA in response to osteogenic induction without concomitant increase of mitochondrial mass (Figs. 2A) indicates that the regulations of mtDNA copy number and mitochondrial mass are not coupled during differentiation. Nevertheless, in our study, mitochondrial mass was measured by a commonly used fluorescent dye, NAO, which binds specifically to cardiolipin on the mitochondrial inner membrane. It might be possible that during osteogenic differentiation of hMSCs, mitochondrial biogenesis was intensified in conjunction with minor changes in the cardiolipin content, but the protein levels of respiratory enzyme complexes, oxygen consumption rate and mRNA levels of three mitochondrial biogenesis-associated genes including Pol γ, mtTFA and PGC-1α[22-24] were increased (Fig. 2). One possible reason is that during osteogenic differentiation of hMSCs, mitochondrial ultrastructure is altered to form more cristae protruding into the matrix to accommodate more respiratory enzyme complexes. Lonergan *et al*. [5] showed that the stem cell property is associated with the peri-nuclear arrangement of mitochondria in adult monkey stromal stem cells. Consistently, we observed peri-nuclear distribution of mitochondria in the early phase of osteogenic induction and an evenly-distributed pattern was resumed after two weeks of differentiation (unpublished data).

Although oxidative phosphorylation is the most efficient way to generate ATP, it is not always the best way for cells to fuel themselves. Early in the 1930s, Otto Warburg [25] first proposed that cancer cells rely primarily on anaerobic glycolysis instead of oxidative phosphorylation, which is termed Warburg effect. This has been extensively studied to understand the metabolic aberrations of cancer cells. Similarly, the metabolic pattern of stem cells may also be different from that of terminally differentiated cells. Kondoh *et al.* [4] demonstrated that the highly proliferative capacity of murine ESCs is closely associated with high activity of glycolytic enzymes, elevated glycolytic flux and low mitochondrial oxygen consumption. In the present study, we observed that hMSCs expressed higher levels of glycolytic enzymes such as GPI, PFK and PDK and lower level of PDH (Fig. 3A). Another index for anaerobic metabolism, lactate production rate, was also higher in undifferentiated hMSCs than in ost2w (Fig. 3B), indicating a high glycolytic activity. Together with the findings of the increase of mitochondrial biogenesis, it is evident that an energy production switch from anaerobic glycolysis to mitochondrial respiration and oxidative phosphorylation occurred during the osteogenic differentiation of hMSCs. An overall increase of intracellular ATP content (Fig. 3C) indicates that energy burst is essential for the hMSCs to go through the differentiation process. In addition, hMSCs were more

vulnerable to glycolytic inhibitor-induced cell death (Figs. 4A and 4B), which suggests that hMSCs indeed rely more on glycolysis in comparison with the differentiated osteoblasts, ost2w. The lower levels of ATP content (Fig. 3C) and mitochondrial biogenesis of hMSCs may reflect the quiescence-maintaining property of stem cells. It seems that hMSCs prefer to produce energy by glycolysis to avoid the production of ROS, the deleterious byproducts of aerobic metabolism.

Mitochondria are the major source of endogenous ROS in human cells. The electron leaked out from the electron transport chain contributes to the production of mitochondrial ROS. In the present study, intracellular H_2O_2 and $O_2^{\cdot-}$ levels were significantly reduced (Fig. 5A), although mitochondrial respiration was enhanced during osteogenic differentiation of hMSCs. The possibility that the reduction of intracellular ROS was due to ascorbic acid added in the osteogenic induction medium was excluded by the observation that ROS was not decreased simply by adding ascorbic acid to the culture medium (day 6: 89.5 ± 5.6%). On the contrary, the intracellular H_2O_2 levels in cells treated with dexamethasone and β-glycerol phosphate without ascorbic acid was lower (day 6: 61.4 ± 9.8%) than that of cells treated with ascorbic acid alone. However, the H_2O_2 level was not as low as that found when osteogenic induction was induced (Fig. 5A; day 6: 40.3 ± 3.4%). These findings suggest that the antioxidative effects are mainly contributed by differentiation rather than by ascorbic acid. On the other hand, the time-dependent upregulation of catalase and MnSOD upon osteogenic induction (Figs. 5B and 5C) was closely correlated with the decrease of intracellular ROS. Results from measurement of catalase and total SOD activities (Figs. 6A and 6B) as well as cell viability assay after exogenous ROS treatment (Figs. 6C and 6D) demonstrate that differentiated osteoblasts had relatively higher antioxidative capacity. This finding suggests that during osteogenic differentiation, a coordinated regulation between mitochondrial biogenesis and antioxidant defense systems is orchestrated to prevent the accumulation of ROS when aerobic metabolism of mitochondria becomes dominant. Another effective regulator, uncoupling protein 2 (UCP2), might also contribute to the alterations of mitochondrial ATP synthesis and ROS generation [26]. We found that the mRNA expression level of UCP2 was increased with a peak level on day 21 after osteogenic induction (data not shown). Further experiments are needed to determine whether altered expression of UCP2 is related to the dramatic changes of mitochondrial respiratory function and intracellular ROS in the differentiation process of hMSCs.

Recent studies have indicated that cell differentiation is also influenced by ROS. Su *et al*. [27] showed that ROS enhanced vascular smooth muscle cell differentiation through the p38/MAPK-dependent pathway. On the contrary, Mody *et al*. [28] reported that ROS inhibited the differentiation of bone preosteoblast cell line MC3T3-E1. We found that sublethal doses of exogenous H_2O_2 significantly reduced the ALP activity and the mRNA expression level of the osteoblast-specific maker gene, Cbfa-1 (Figs. 7A and 7C). On the other hand, oligomycin also reduced the ALP activity and Cbfa-1 expression

(Figs. 7B and 7C), suggesting the importance of mitochondrial respiratory function during osteogenic differentiation. However, since oligomycin not only inhibits ATP synthase activity but also increases the production of intracellular ROS, further studies need to be carried out to delineate whether oligomycin or ROS would be the major inhibitor to osteogenic differentiation of hMSCs. We speculate that a well-organized regulatory circuit must be turned on to control mitochondrial biogenesis and antioxidative defense systems to create a proper intracellular environment for hMSC differentiation.

We observed significant decrease in lactate production rate and increase in the protein expression of MnSOD 7 days after osteogenic induction of hMSCs from five different donors (Supplementary Figure 1). These observations support that there is coordination between increase of mitochondrial respiration and upregulation of antioxidant enzymes during osteogenic differentiation of hMSCs.

It is also important to identify the messengers that orchestrate the coordinated expression of the genes encoding respiratory enzymes and antioxidant enzymes. Recently, St-Pierre *et al.* [29] demonstrated that PGC-1α is required for not only mitochondrial biogenesis but also the induction of several ROS-detoxifying enzymes including MnSOD and GPx-1 after exposure of the cells to an oxidative stressor. We also observed an upregulation of PGC-1α during osteogenic differentiation of hMSCs. Further efforts should be made to investigate whether PGC-1α is regulated by osteogenesis-specific genes to coordinate mitochondrial biogenesis and antioxidant enzyme expression. Interestingly, we noticed that the mRNA expression levels of mtTFA, MnSOD and catalase were also upregulated during hepatogenic differentiation while only mtTFA and catalase, but not MnSOD, levels were increased during chondrogenic differentiation of hMSCs (unpublished data). These results suggest that the coordinated changes in mitochondrial biogenesis and antioxidant enzymes are a general regulatory mechanism during differentiation of hMSCs but lineage-specific gene regulation still exists.

In summary, we demonstrated that alterations in mitochondrial biogenesis and antioxidant enzymes are well coordinated during osteogenic differentiation of hMSCs. Understanding the roles of mitochondria and ROS during cell differentiation will facilitate the optimization of *in vitro* differentiation protocols by adjusting biochemical properties such as energy production or redox status of stem cells for better design of cell therapy. Besides, the energy production profile or bioenergetic signature dictated by mitochondrial biogenesis may also serve as an index to identify stem cells of better quality in a given cell pool.

ACKNOWLEDGEMENT

This work was supported by grants from the National Science Council of Taiwan (NSC95-2320-B-010-011 and NSC95-2475-B-075-002-MY3), a project of "Aim for Top University Plan" sponsored by the Ministry of Education, Executive Yuan, Taiwan, and by intramural grant from Taipei Veterans General Hospital (V96E1-006).

REFERENCES

1. da Silva Meirelles L, Chagastelles PC, Nardi NB. Mesenchymal stem cells reside in virtually all post-natal organs and tissues. J Cell Sci 2006;119:2204–2213.
2. Giordano A, Galderisi U, Marino IR. From the laboratory bench to the patient's bedside: an update on clinical trials with mesenchymal stem cells. J Cell Physiol 2007;211:27–35.
3. Nesti C, Pasquali L, Vaglini F et al. The role of mitochondria in stem cell biology. Biosci Rep 2007;27:165–171.
4. Kondoh H, Lleonart ME, Nakashima Y et al. A high glycolytic flux supports the proliferative potential of murine embryonic stem cells. Antioxid Redox Signal 2007;9:293–299.
5. Lonergan T, Brenner C, Bavister B. Differentiation-related changes in mitochondrial properties as indicators of stem cell competence. J Cell Physiol 2006;208:149–153.
6. DiMauro S, Schon EA. Mitochondrial respiratory-chain diseases. N Engl J Med 2003;348:2656–2668.
7. Brandon MC, Lott MT, Nguyen KC et al. MITOMAP: a human mitochondrial genome database-2004 update. Nucleic Acids Res 2005;33:D611–D613.
8. Wallace DC. Mitochondrial diseases in man and mouse. Science 1999;283:1482–1488.
9. Adam-Vizi V, Chinopoulos C. Bioenergetics and the formation of mitochondrial reactive oxygen species. Trends Pharmacol Sci 2006;27:639–645.
10. Lu CY, Lee HC, Fahn HJ et al. Oxidative damage elicited by imbalance of free radical scavenging enzymes is associated with large-scale mtDNA deletions in aging human skin. Mutat Res 1999;423:11–21.
11. Valko M, Leibfritz D, Moncol J et al. Free radicals and antioxidants in normal physiological functions and human disease. Int J Biochem Cell Biol 2007;39:44–84.
12. Cadenas E, Davies KJ. Mitochondrial free radical generation, oxidative stress, and aging. Free Radic Biol Med 2000;29:222–230.
14. Balaban RS, Nemoto S, Finkel T. Mitochondria, oxidants, and aging. Cell 2005;120:483–495.
16. Lee OK, Kuo TK, Chen WM et al. Isolation of multipotent mesenchymal stem cells from umbilical cord blood. Blood 2003;103:1669–1675.
17. Lee OK, Ko YC, Kuo TK et al. Fluvastatin and lovastatin but not pravastatin induce neuroglial differentiation in human mesenchymal stem cells. J Cell Biochem 2004;93:917–928.
18. Lee KD, Kuo TK, Whang-Peng J et al. In vitro hepatic differentiation of human mesenchymal stem cells. Hepatology 2004;40:1275–1284.
19. Shih YR, Chen CN, Tsai SW et al. Growth of mesenchymal stem cells on electrospun type I collagen nanofibers. Stem Cells 2006;24:2391–2397.
20. Lee CF, Chen YC, Liu CY et al. Involvement of protein kinase C delta in the alteration of mitochondrial mass in human cells under oxidative stress. Free Radic Biol Med 2006;40:2136–2146.
21. Spitz DR, Oberley LW. An assay for superoxide dismutase activity in mammalian tissue homogenates. Anal Biochem 1989;179:8–18.
22. Cho YM, Kwon S, Pak YK et al. Dynamic changes in mitochondrial biogenesis and antioxidant enzymes during the spontaneous differentiation of human embryonic stem cells. Biochem Biophys Res Commun 2006;348:1472–1478.

23. Bavister BD. The mitochondrial contribution to stem cell biology. Reprod Fertil Develop 2006;18:829–838.
24. Moyle G. DNA polymerase gamma, the mitochondrial replicase. Annu Rev Biochem 2004;73:293–320.
25. Gleyzer N, Vercauteren K, Scarpulla RC. Control of mitochondrial transcription specificity factors (TFB1M and TFB2M) by nuclear respiratory factors (NRF-1 and NRF-2) and PGC-1 family coactivators. Mol Cell Biol 2005;25:1354–1366.
26. Kelly DP, Scarpulla RC. Transcriptional regulatory circuits controlling mitochondrial biogenesis and function. Genes Dev 2004;18:357–368.
27. Warburg O. On the origin of cancer cells. Science 1956;123:309–314.
28. Krauss S, Zhang SY, Lowell BB. The mitochondrial uncoupling-protein homologues. Nat Rev Mol Cell Biol 2005;6:248–261.
29. Su B, Mitra S, Gregg H et al. Redox regulation of vascular smooth muscle cell differentiation. Circ Res 2001;89:39–46.
30. Mody N, Parhami F, Sarafian TA et al. Oxidative stress modulates osteoblastic differentiation of vascular and bone cells. Free Radic Biol Med 2001;31:509–519.
31. St-Pierre J, Drori S, Uldry M et al. Suppression of reactive oxygen species and neurodegeneration by the PGC-1 transcriptional coactivators. Cell 2006;127:397–408.

Figure 1. Osteogenic differentiation of hMSCs. Representative images of undifferentiated hMSCs (A) and 3 week-differentiated osteoblasts (B), which demonstrated flattened and polygonal shapes and showed positive signals for ALP activity. (C) Increase of the ALP activity of hMSCs during osteogenic differentiation. (D) Increase in the expression levels of four osteoblast-specific marker genes, Cbfa-1, osteocalcin, osteonectin and osteopontin. All data were obtained from three independent experiments, expressed as means ± SD and analyzed by nonparametric Mann-Whitney U test. (*, $p < 0.05$)

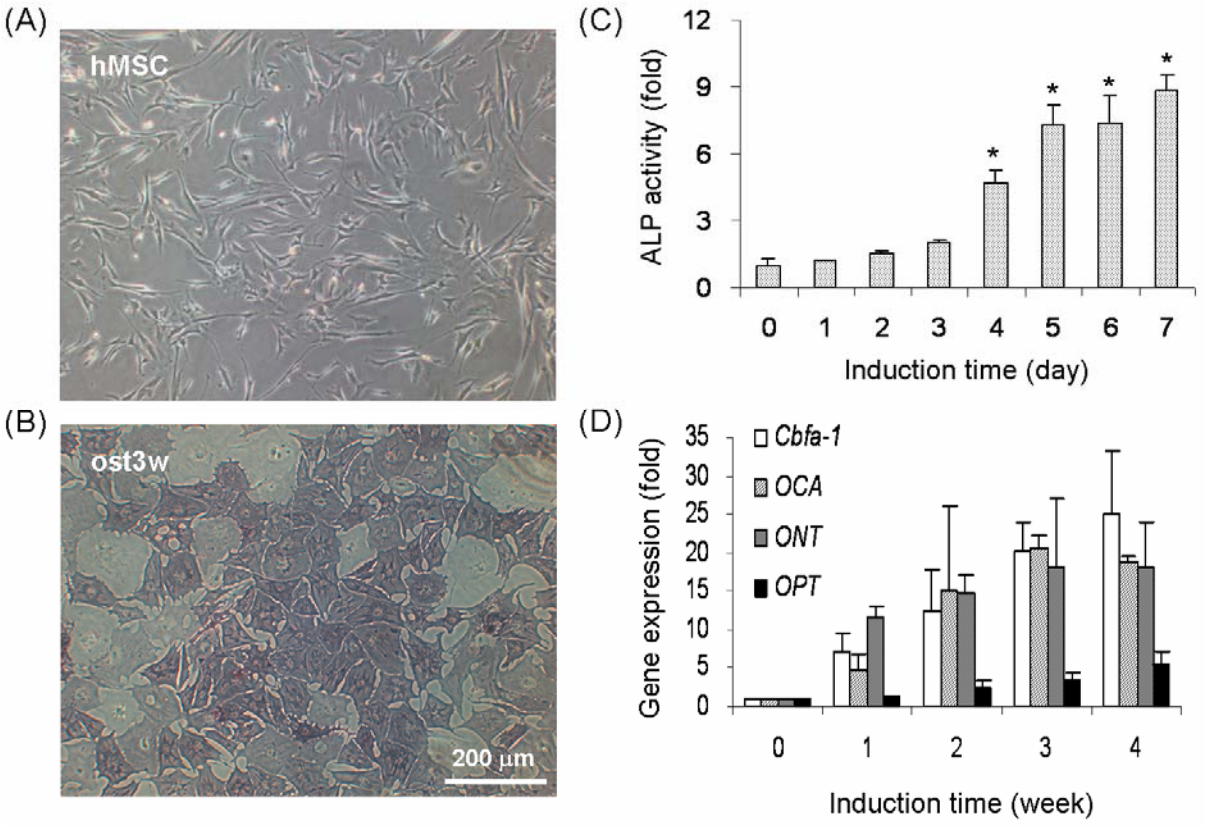

Figure 2. Augmentation of mitochondrial biogenesis and respiration during osteogenic differentiation of hMSCs. (A) Dynamic changes of mitochondrial mass and mtDNA copy number. (B) Increase in the protein levels of respiratory enzymes in 2-week differentiated hMSCs, ost2w. Folds of increase are shown. (C) Enhancement of oxygen consumption rate in ost2w. (D) Gradual increase of the mRNA expression levels of three crucial mitochondrial biogenesis-associated genes, mtTFA, Pol γ and PGC-1α All data were obtained from three independent experiments, expressed as means ± SD and analyzed by nonparametric Mann-Whitney U test. (* and #, $p < 0.05$)

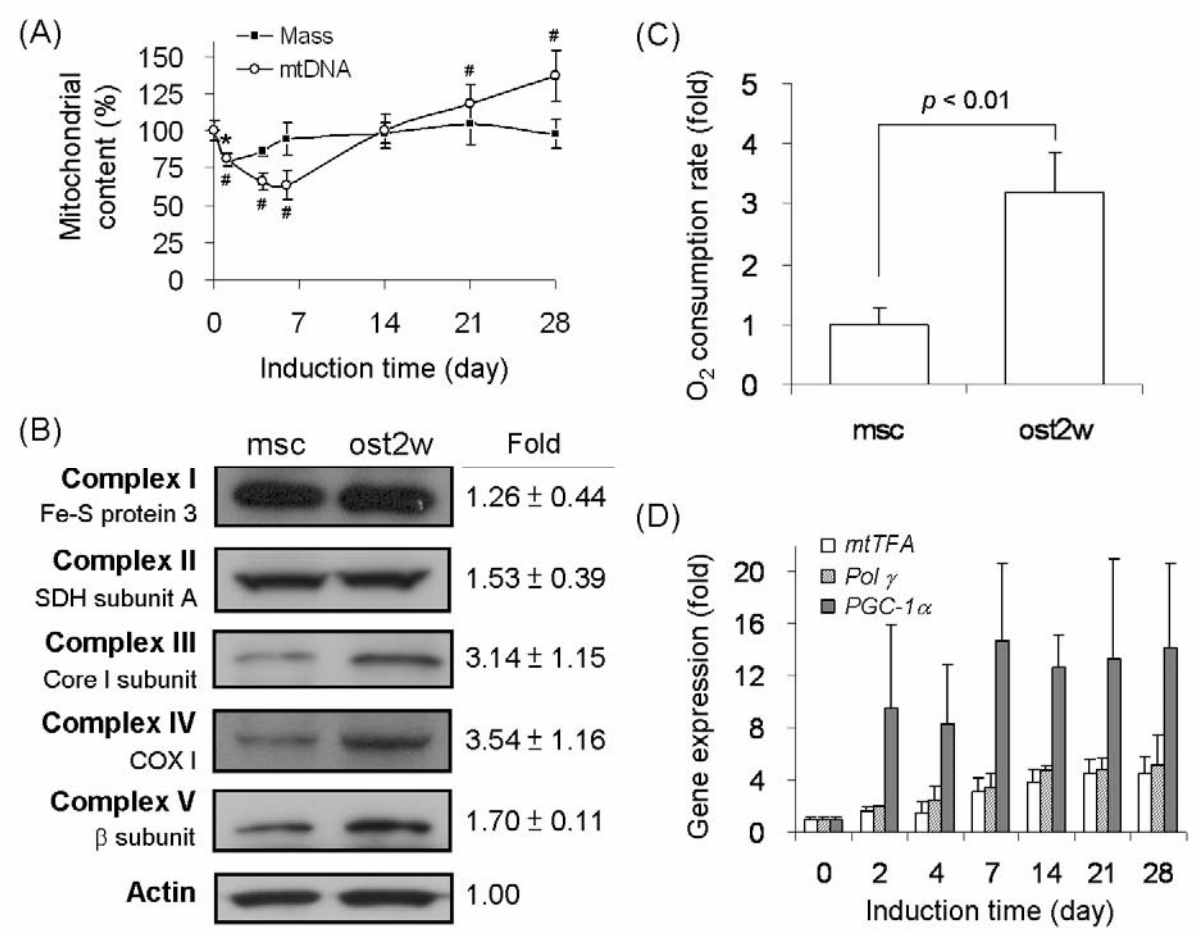

Figure 3. Suppression of glycolytic enzymes and lactate production rate during osteogenic differentiation of hMSCs. (A) Decrease in the protein levels of glycolytic enzymes such as GPI and PFK, and an increase of PDH and decrease of its inhibitory kinase PDK in ost2w. (B) Decrease of lactate production rate in ost2w. (C) Increase of the intracellular ATP content from the fourth day of induction. All data were obtained from three independent experiments, expressed as means ± SD and analyzed by nonparametric Mann-Whitney U test. (*, $p < 0.05$).

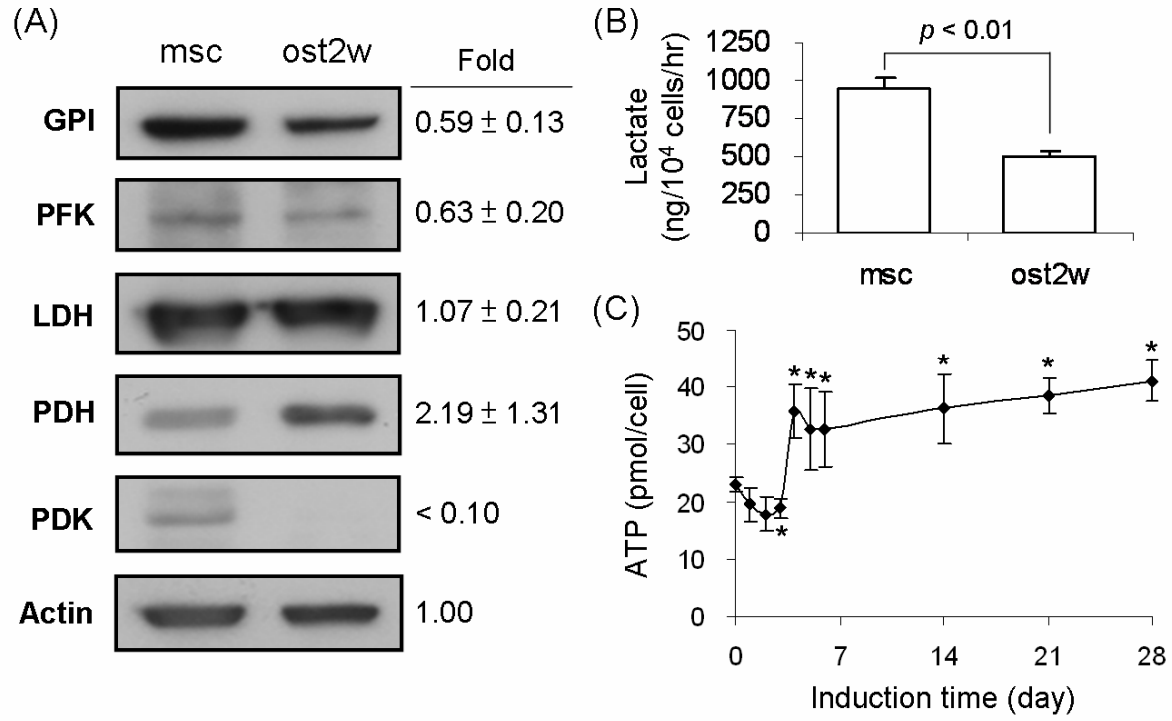

Figure 4. Extent of dependence on aerobic and anaerobic metabolism of hMSCs and ost2w. (A, B) Lower cell viability of hMSCs after treatment with the glycolytic inhibitor iodoacetamide or 2-deoxy-glucose. (C, D) Lower cell viability of ost2w after treatment with mitochondrial inhibitor antimycin A or oligomycin. All data were obtained from three independent experiments, expressed as means ± SD and analyzed by nonparametric Mann-Whitney U test. (*, $p < 0.05$)

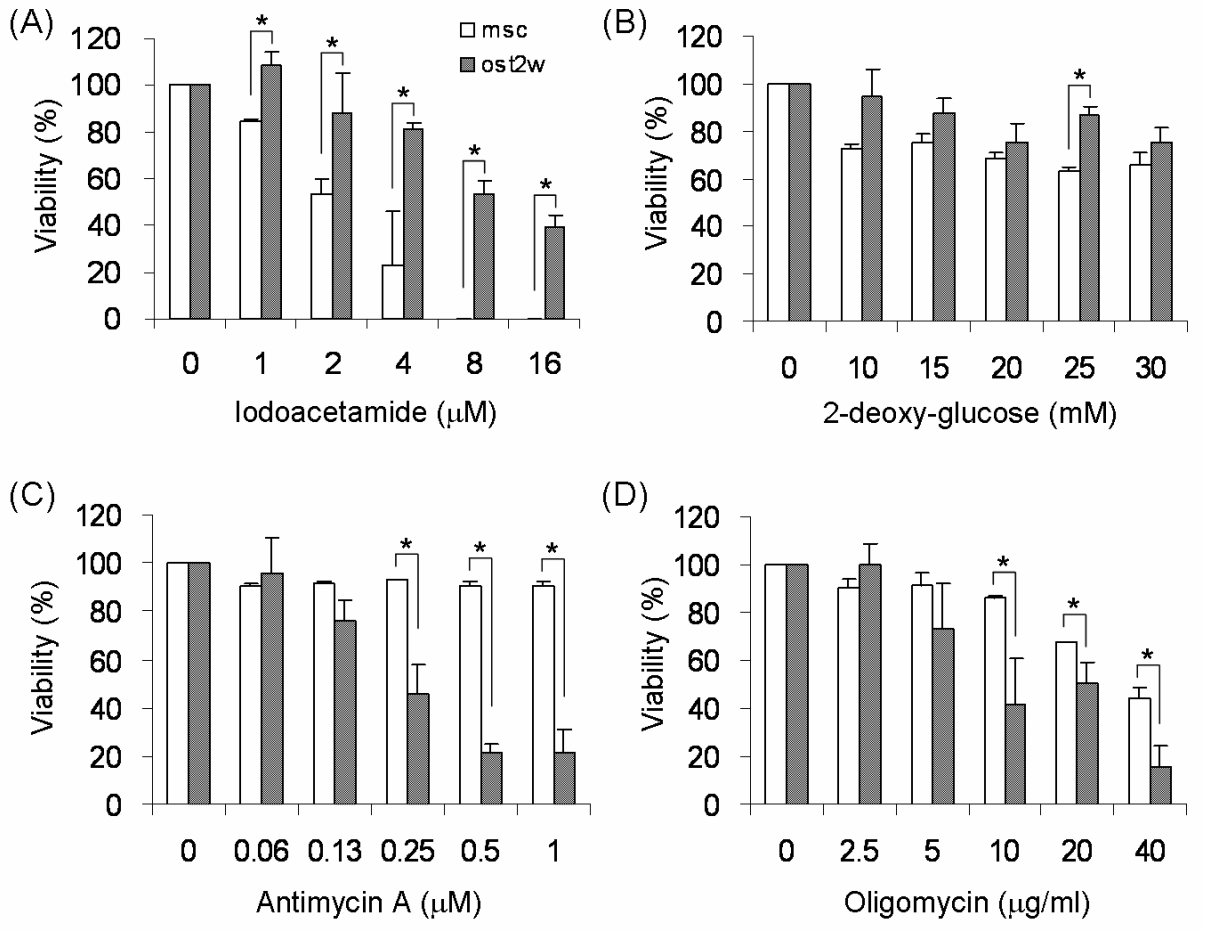

Figure 5. Decrease of intracellular ROS levels and increase of the expression of antioxidant enzymes during osteogenic differentiation of hMSCs. (A) Decline of intracellular levels of H_2O_2 and $O_2^{\cdot-}$ in the early phase of osteogenic induction. (B, C) Time-dependent increase of the protein amounts of catalase and MnSOD, but not Cu/ZnSOD, as shown in the indicated blots and their relative intensities. All data were obtained from three independent experiments, expressed as means ± SD and analyzed by nonparametric Mann-Whitney U test. (* and #, $p < 0.05$)

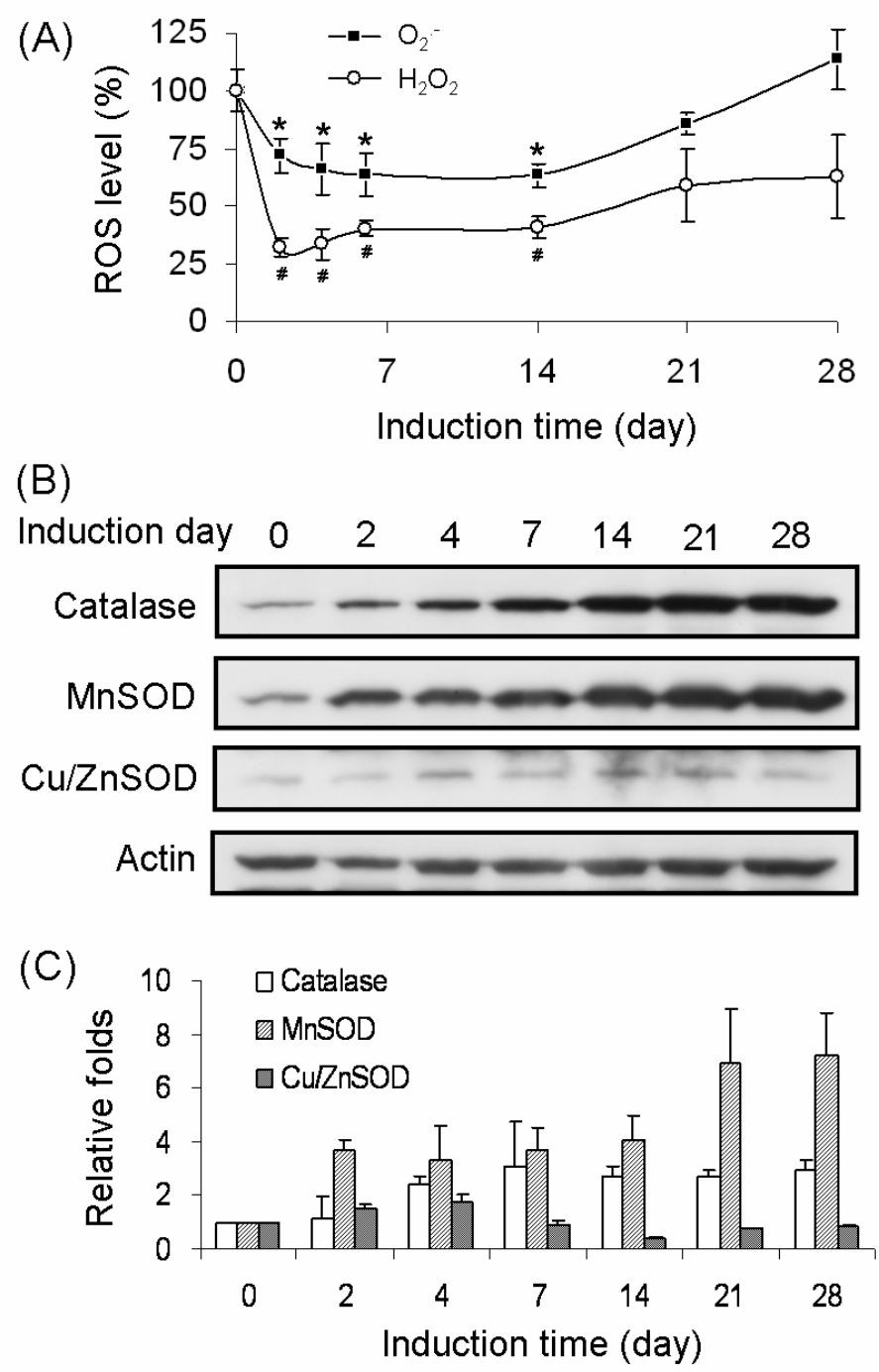

Figure 6. Increase of antioxidative capacity of differentiated osteoblasts. (A, B) Increase in the activities of catalase and total SOD in ost2w. (C, D) Reduction in the cell viability of hMSCs compared with differentiated ost2w upon treatment with H_2O_2 or menadione. All data were obtained from three independent experiments, expressed as means ± SD and analyzed by nonparametric Mann-Whitney U test. (*, $p < 0.05$)

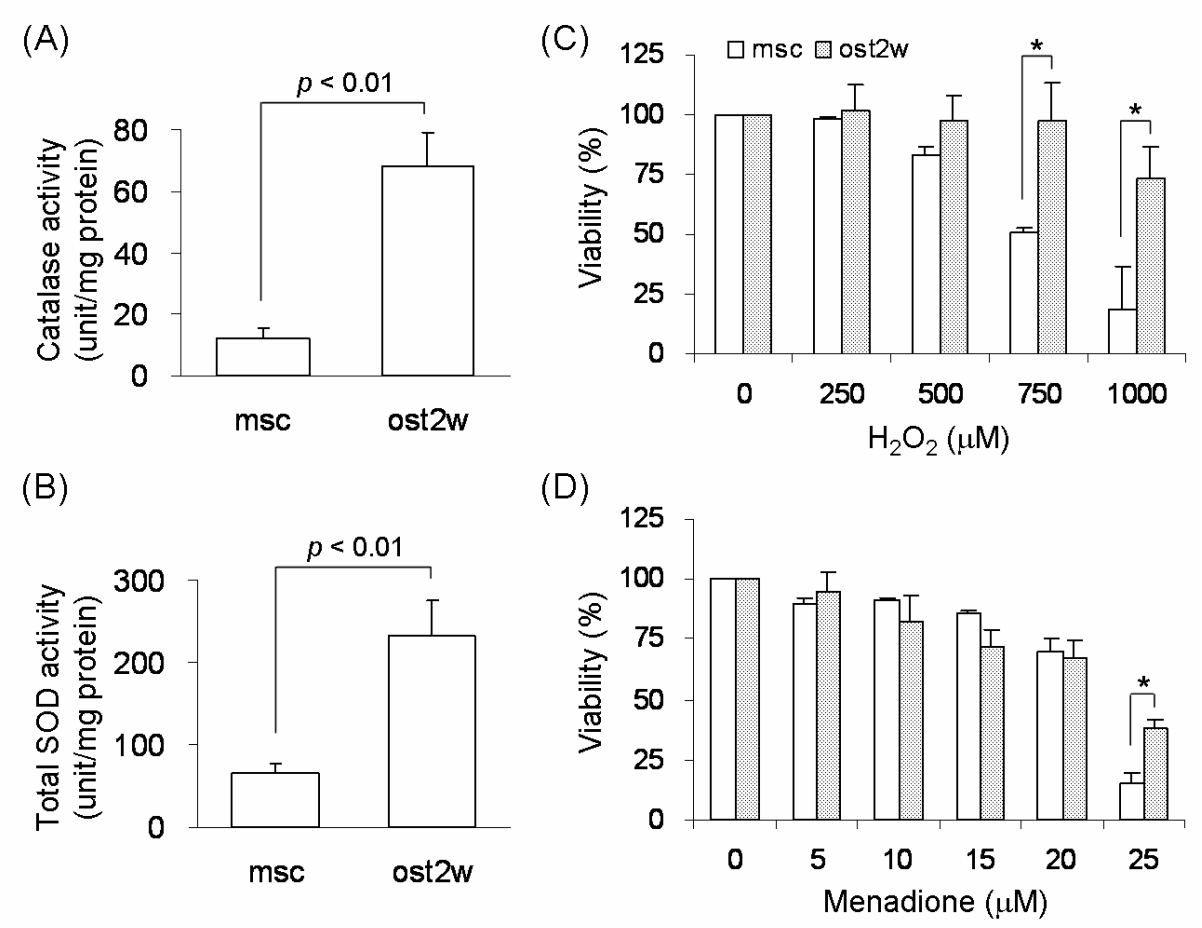

Figure 7. Inhibitory effects of H_2O_2 and oligomycin on osteogenic differentiation of hMSCs. (A) Reduction of the ALP activity of hMSCs after treatment with 125-500 μM H_2O_2. (B) Reduction of the ALP activity of hMSCs after treatment with 2.5 μg/ml oligomycin. (C) Reduction of the Cbfa-1 mRNA expression level after treatment with either H_2O_2 or oligomycin. All data were obtained from three independent experiments, expressed as means ± SD and analyzed by nonparametric Mann-Whitney U test (*, $p < 0.05$).

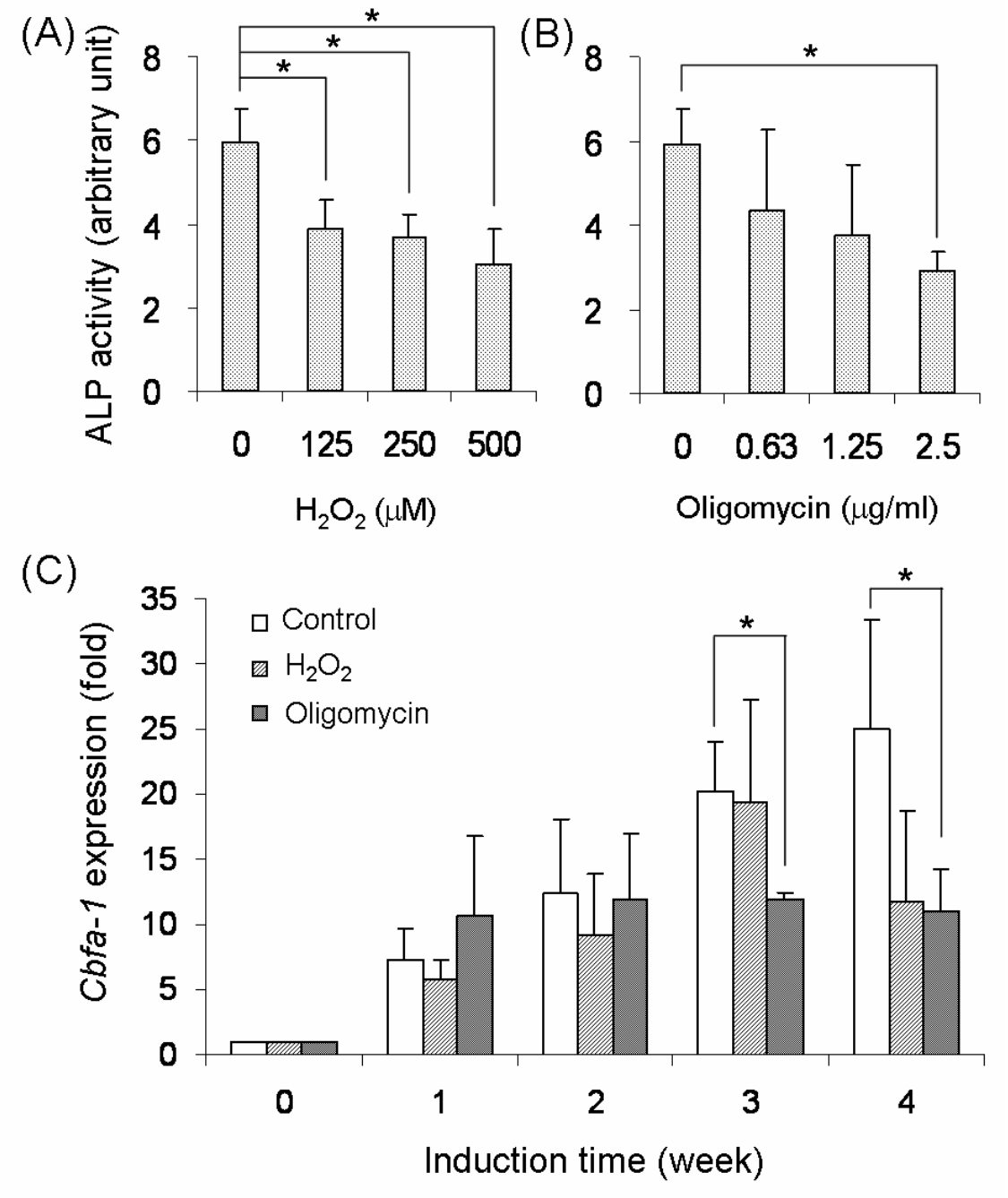

Coordinated Changes of Mitochondrial Biogenesis and Antioxidant Enzymes during Osteogenic Differentiation of Human Mesenchymal Stem Cells

Chien-Tsun Chen, Yuru V. Shih, Tom K. Kuo, Oscar K. Lee and Yau-Huei Wei

Stem Cells published online Jan 24, 2008;
DOI: 10.1634/stemcells.2007-0509